Correlated structural distributions in silica glass

Ted M. Clark and Philip J. Grandinetti*
Department of Chemistry, The Ohio State University, 120 West 18th Avenue, Columbus, Ohio 43210-1173, USA

Pierre Florian
CNRS-CRMRT, 1D Av. de la Recherche Scientifique, 45071 Orléans Cedex 2, France

Jonathan F. Stebbins
Department of Geological and Environmental Sciences, Stanford University, Stanford, California 94305-2115, USA
(Received 27 February 2004; revised manuscript received 4 June 2004; published 18 August 2004)

The two-dimensional ^{17}O dynamic-angle spinning solid-state nuclear magnetic resonance spectrum of silica glass produced from the melt was measured. From this spectrum a three-dimensional histogram correlating ^{17}O chemical shift, quadrupolar coupling constant, and quadrupolar coupling asymmetry parameter for the bridging oxygen was obtained. Using existing correlations between NMR parameters and local structure, the distribution in quadrupolar coupling parameters was mapped into two-dimensional histograms correlating the Si-O-Si angle with Si-O distance, the Si-O-Si angle with Si-Si distance, and the Si-O distance with Si-Si distance. While the peak values for the Si-O-Si angle, the Si-O distance, and Si-Si distance distributions, at 147°, 1.59 Å, and 3.05 Å, respectively, are consistent within the precision of the NMR measurement with previous diffraction studies, the distribution widths are narrower than previous diffraction studies. The two-dimensional histogram reveals an unexpected strong positive correlation between the Si-O-Si angle and Si-O distance in the glass, running opposite to the trend generally found in crystalline silica polymorphs.

DOI: 10.1103/PhysRevB.70.064202 PACS number(s): 61.43.Fs, 61.18.Fs

I. OVERVIEW

Silica is the archetypical glass former and is of significant scientific and technological importance in several disciplines. Despite this importance, many fundamental aspects of its atomic level structure remain unknown. In 1932, Zachariasen[1] predicted that the structure of silica glass consisted of well-defined corner-sharing SiO_4 tetrahedra connected in a continuous infinite three-dimensional network having no long-range order. The interconnection of two tetrahedra involves a Si-O-Si bond angle and two dihedral angles; the variation in these angles is considered to be one of the main sources of disorder in a conventional melt quenched silicate glass. Shortly afterward, these ideas were experimentally confirmed by Warren[2] using x-ray diffraction techniques.

In 1969, Mozzi and Warren[3] published the often cited Si-O-Si bond angle probability distribution for silica glass, claiming that it peaked near 144°, had a full width at half maximum of 37°, and was skewed towards lower angles. Recently, Neuefeind and Liss[4] reanalyzed high-energy x-ray[5] and neutron[6,7] diffraction data of silica glass without the assumption of randomly distributed dihedral angles to obtain a Si-O-Si bond angle distribution that is nearly half the width found by Mozzi and Warren.

Silicon-29 magic-angle spinning (MAS) nuclear magnetic resonance (NMR) has provided another means of obtaining the Si-O-Si bond angle distribution[8–12] with varying success. A correlation between the ^{29}Si chemical shift of an SiO_4 tetrahedra and the average of its four Si-O-Si angles in the second coordination sphere has been used to map the ^{29}Si MAS NMR lineshape into the Si-O-Si distribution. Unfortunately, many Si-O-Si angles can map to the same silicon-29 chemical shift in the averaging process, making this is a rather complicated and suspect process for obtaining Si-O-Si angle distributions.[10] Additionally, for reasons of spectral overlap this approach becomes intractable for multi-component silicate glasses and its application, like diffraction techniques, has also been limited to SiO_2 glass.

A better approach to measuring Si-O-Si bond angle distributions is to use methods that provide a more detailed and direct measurement of the local environment around oxygen. Unfortunately, the information obtainable from x-ray absorption spectroscopies has been limited for light backscattering atoms like oxygen.[13] In contrast, solid-state ^{17}O NMR, specifically, the ^{17}O quadrupolar coupling and chemical shift parameters, provide a simple and direct probe of the electronic structure, and is well suited for measuring the local structure around bridging oxygen.[14–23] In 1983, Geissberger and Bray[24] obtained the first ^{17}O NMR spectrum of silica glass. From their analysis, they concluded that the average Si-O-Si bond angle was 144° and its distribution ranged from 130° to 180°. Their data analysis, however, was limited since it relied on fitting heavily overlapping NMR spectra, which required an assumption of a Gaussian distribution in NMR parameters. While this has been a common practice in solid-state NMR analyses of glasses, there generally has been no justification for this other than the central limit theorem. Additionally, such analyses are forced to assume specific (typically random) correlations between NMR parameters. The development of two-dimensional NMR methods that separate and correlate anisotropic and isotropic lineshapes[25–27] has helped eliminate the need for these assumptions.[28,29] In 1992, Farnan *et al.*[30] first demonstrated how the distribution of ^{17}O NMR

parameters can be measured in a silicate glass using two-dimensional dynamic-angle spinning (DAS) NMR, without any assumptions about the shape of the NMR parameter distributions. Additionally, they demonstrated that the ^{17}O quadrupolar coupling parameter distribution can, in principle, be mapped into the one-dimensional Si-O-Si bond angle distribution in the glass.

In this work we have combined the recent development of RAPT (Rotor Assisted Population Transfer)[31–33] for enhancing sensitivity in solid-state ^{17}O NMR with high resolution DAS to obtain the complete three-dimensional distribution of ^{17}O chemical shift, quadrupolar coupling constant, and quadrupolar asymmetry parameter for the bridging oxygen resonances in silica glass. Combining this result with recently improved relationships[23] between ^{17}O quadrupolar coupling parameters and the local structure around bridging oxygen allows us to obtain the one-dimensional distributions in Si-O-Si angle, Si-O distance, and Si-Si distance, and, for the first time, two-dimensional distribution correlating Si-O-Si angle with Si-O distance, Si-O-Si angle with Si-Si distance, and Si-O distance with Si-Si distance.

II. METHODS

A. Sample preparation

Silica gel was first prepared by reacting 48.6% ^{17}O-labeled H_2O (Cambridge Isotope Labs) with $SiCl_4$. The gel was dried at 1000°C in high-purity, gettered argon, then welded under vacuum into a molybdenum tube. This was heated at 1850°C for 30 minutes under Ar in a graphite-element furnace. The sample was cooled through the glass transition at approximately 40 deg./min. A clear, somewhat bubbly, crystal-free glass was recovered. An analysis by electron microprobe did not reveal any contamination of the glass with Mo, at a detection limit of 0.03 wt%.

B. NMR spectroscopy

The RAPT (Rotor Assisted Population Transfer)[31–33] enhanced two-dimensional ^{17}O dynamic-angle spinning spectrum of silica glass is shown in Fig. 1. Also shown in Fig. 1 are the one-dimensional projections onto the MAS and isotropic dimensions, along with selected experimental cross sections and best fit simulations on the right.

All ^{17}O NMR experiments were performed at 9.4 T on a Chemagnetics CMX II spectrometer using a modified version of a homebuilt DAS probed described earlier.[34] The sample was contained in a silicon nitride rotor with a 4 mm diameter. Experiments were performed at ambient temperature with a sample spinning rate of approximately 15 kHz, and chemical shift data referenced with respect to the ^{17}O resonance in tap water. A recycle delay of 60 seconds for ^{17}O was determined using a saturation recovery experiment under MAS conditions. The DAS angle pair (38.38°, 79.19°) was employed in removing the second order anisotropic broadenings, while detection was carried out at 54.74° to eliminate all chemical shift anisotropy contributions to the

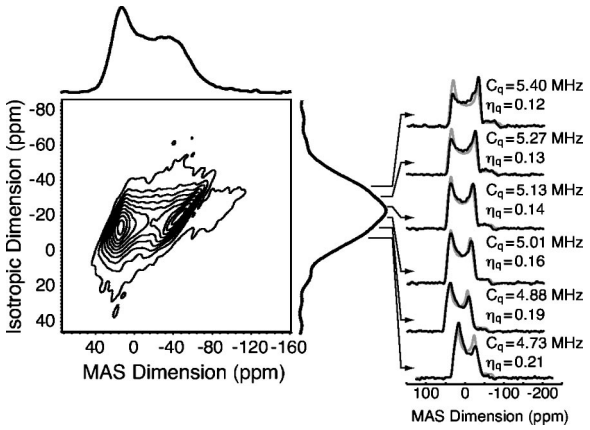

FIG. 1. Experimental two-dimensional ^{17}O RAPT/MAS-detected DAS spectrum of in SiO_2 glass at 9.4 T along with experimental one-dimensional projections onto the MAS and isotropic dimensions. Frequency axes are referenced from $H_2^{17}O$. The contour lines are drawn at levels of 5, 15, 25, 35, 45, 55, 65, 75, 85, 95 percent of the maximum intensity. Shown on the right are selected experimental cross sections along with best fit simulations (in gray).

anisotropic lineshape.[19,35] The DAS pulse sequence was preceded with a Gaussian RAPT preparation[32] to improve signal to noise by a factor of 2.4. The optimized RAPT parameters were obtained at 38.38°. These include a Gaussian pulse width of 9 μsec, divided into 15 increments of 0.6 μseconds to obtain a Gaussian-shaped pulse (σ=1.8 μsec) with an off-resonance frequency of ±525 kHz. The RAPT Gaussian pulse pair was repeated 400 times before the MAS-detected DAS sequence. The $\pi/2$ pulse widths of 8 μsec, 7.2 μsec, and 7.5 μsec were used for the angles 38.38°, 79.19°, and 54.74°, respectively. The DAS echo was shifted[36] by 1 millisecond, an integer number of rotor periods, using a π pulse of 15 μsec. The t_1 dimension was zero-filled to 256 points and no apodization was applied to this dimension to preserve the highest possible resolution.

Additionally, ^{29}Si MAS spectra were collected at 14.1 T and at a spinning rate of 18 kHz, with a Varian/Chemagnetics 3.2 mm T3 type probe. The ^{29}Si NMR spectrum collected with a 30° tip angle and a delay of 5000 sec was similar to that reported by Gladden *et al.*[12] It was approximately Gaussian in shape, centered at -111.2 ± 0.5 ppm with a FWHM of 12 ± 0.5 ppm. Silicon-29 spin-lattice relaxation followed a power-law behavior as previously reported for other samples,[37] but could be approximated with a T_1 of at least 1400 seconds.

When fitting the 2D ^{17}O DAS spectrum we assume that each ω_1 cross section contains the anisotropic second-order quadrupolar central transition lineshape of a single site. That is, the subset of the oxygen atoms resonating at each ω_1 value has such a narrow range of local structural variations that their NMR parameters are nearly identical. Selected cross-sections shown in Fig. 1 along with best fit "single site" lineshapes are in good agreement, supporting this assumption. The fit of the anisotropic lineshape in each cross section is additionally constrained to have the total isotropic shift, δ_{iso}, constrained by each cross-section's position in ω_1, that is,

$$\omega_1 = \delta_{iso} = \delta_{cs} + \delta_q, \quad (1)$$

where δ_{cs} is the isotropic chemical shift, and δ_q is the isotropic second-order quadrupolar shift.[27] Since certain parameters describing a given cross section have zero covariance with parameters describing other cross sections, we have adopted an algorithm for fitting the 2D spectrum that performs two least squares fits: one inside the other. An "inner" least squares fit is performed on each 1D cross section. The individual best fit chi squared values of each cross section are added to get the total chi squared for the 2D spectrum. An "outer" least squares fit is then performed using the total chi squared for the 2D spectrum with parameters that were constant during the "inner" least squares fit becoming fit variables during the "outer" least squares fit. Two different approaches were taken when fitting the data in Fig. 1. In the first approach, each cross section was fit for the quadrupolar coupling constant, C_q, quadrupolar asymmetry parameter, η_q, and area with fixed constraints of Gaussian broadening and total isotropic shift, $\delta_{iso}=\omega_1$. Gaussian broadening was then varied as part of the "outer" least squares fit to obtain the minimum total chi squared. In the second approach, we fit each cross section for C_q and area with fixed constraints of Gaussian broadening, total isotropic shift, $\delta_{iso}=\omega_1$, and a linear relationship between C_q and η_q. The slope and intercept of the linear relationship as well as Gaussian broadening were varied as part of the "outer" least squares fit to obtain the minimum total chi squared. The best-fit distributions of C_q and chemical shift were virtually unaffected by the introduction of the linear correlation between C_q and η_q, whereas, for η_q significant differences were seen only in the lower intensity cross-section fits, where the uncertainty in η_q is expected to be higher.

III. RESULTS AND DISCUSSION

From the full least-squares analysis of the ^{17}O 2D DAS spectrum, a three-dimensional histogram correlating the ^{17}O chemical shift, δ_{cs}, quadrupolar coupling constant, C_q, and quadrupolar asymmetry parameter, η_q, was obtained. Two-dimensional projections along with corresponding one-dimensional projections of this three dimensional histogram are shown in Fig. 2. The one-dimensional distributions are asymmetric and skewed towards lower chemical shifts, lower (in magnitude) quadrupolar coupling constants, and higher quadrupolar asymmetry parameters. As expected, there are strong correlations among all three NMR parameters as they are all known to be strongly correlated to the local structure around the bridging oxygen (*vide infra*). Although a linear constraint between C_q and η_q was imposed by our least squares fitting procedure to improve convergence for the lower sensitivity cross-sections, eliminating this constraint in the fitting procedure resulted in no significant changes in the correlations.

Over the years we[20–23] and others[14–18] have quantified strong correlations between ^{17}O quadrupolar coupling parameters and the local structure around a Si-O-Si bridging oxygen. The structural features around a bridging oxygen most important in determining the ^{17}O quadrupolar coupling parameters of a bridging oxygen are the nature of the two coordinating network forming cations, the T-O-T′ linkage angle, the T-O bond distances, and the nature and number of coordinating network modifier cations. For Si-O-Si linkages without modifier cations, we further obtained[23] the following

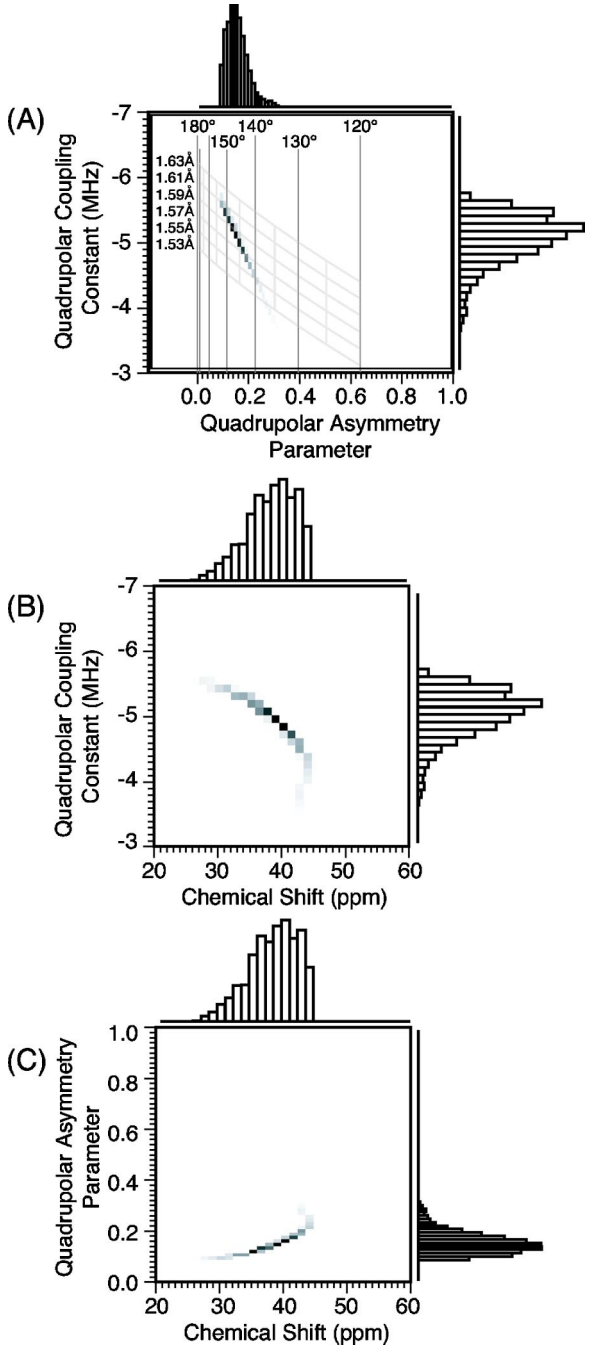

FIG. 2. Two-dimensional histograms along with corresponding one-dimensional projections extracted from the two-dimensional spectrum in Fig. 1 showing the correlation among quadrupolar coupling constant, C_q, asymmetry parameter, η_q, and chemical shift, δ_{cs}. (a) C_q and η_q, (b) C_q and δ_{cs}, and (c) η_q and δ_{cs}. Also shown in (a) is a grid of lines (in gray) obtained from Eqs. (2) and (3) by varying the Si-O distance with the Si-O-Si angle held constant and the Si-O-Si angle with the Si-O distance held constant.

relations between C_q and η_q, and the Si-O-Si angle and Si -O distance:

$$C_q(d_{TO},\Omega) = a'\left(\frac{1}{2} + \frac{\cos\Omega}{\cos\Omega - 1}\right)^{\alpha'} + m_d(d_{TO} - d_{TO}^{\circ}), \quad (2)$$

$$\eta_q(\Omega) = b\left(\frac{1}{2} - \frac{\cos\Omega}{\cos\Omega - 1}\right)^{\beta}, \quad (3)$$

where Ω is the Si-O-Si bond angle and d_{TO} is the average silicon-oxygen bond distance. A least-squares fit of Eqs. (2) and (3) to the experimental values for coesite,[19] cristobalite,[38] and α-quartz[39] as well as the *ab initio* predicted values for ferrierite[40] yields the parameter values $a' = -6.53$ MHz, $\alpha' = 1.80$, $m_d = -12.86$ MHz/Å, $d_{TO}^{\circ} = 1.654$ Å, $b = 4.73$, and $\beta = 1.12$. The precision (i.e., standard deviation) when using these calibrated expressions for predicting Si-O-Si angles, Si-O distances, and Si-Si distances is 4.4°, 0.01 Å, and 0.025 Å, respectively. Using Eqs. (2) and (3) plots of predicted C_q versus η_q as a function of the Si-O distance with the Si-O-Si angle held constant, and as a function of the Si-O-Si angle with the Si-O distance held constant were calculated and are also shown in Fig. 2(a) along with the experimental two-dimensional histogram from SiO_2 glass.

With the aid of Eqs. (2) and (3) the experimental two-dimensional histogram of C_q and η_q in Fig. 2(a) is mapped into the two-dimensional histogram of the Si-O-Si angle versus the Si-O distance shown in Fig. 3(a). From a simple law of cosines calculation, we also obtained the two-dimensional histograms of Si-O distance and Si-O-Si angle versus Si-Si distance in Figs. 3(b) and 3(c), respectively. One-dimensional histograms of the Si-O distance, Si-Si distance, and Si-O-Si angle in silica glass are obtained by projecting the two-dimensional histograms onto their respective axes. Statistical parameters calculated from these distributions are summarized in Table I.

We focus first on the one-dimensional Si-O-Si angle distribution. There is a consensus that the SiO_4 subunits in silica glass are regular tetrahedra and that disorder arises from variability in the Si-O-Si angle distribution. The Si-O-Si angle distribution, also shown in Fig. 4, peaks at 147° with a standard deviation of 3.8°. While this peak position is higher than the 144° found by Mozzi and Warren,[3] it is in agreement with recent high energy x-ray and neutron diffraction studies.[4,5] Although the majority of Si-O-Si angles in low temperature crystalline silicates are near 144°, it has been argued[41] that the range of Si-O-Si angles in silica glass, which quenches in a high temperature structure, would be closer to those found in high temperature silica polymorphs, such as β-quartz and β-cristobalite, where the angles range from 147°–151°. The width of the Si-O-Si angle distribution is significantly narrower than the distribution obtained by Mozzi and Warren,[3] and nearly half the width found by Neuefeind and coworkers.[4,5] Such a difference is not surprising, however, since diffraction, which provides only a direct measure of the Si-O and Si-Si distance distributions, requires modeling and a number of assumptions to construct the Si-O-Si angle distribution. At best, with the proper model and assumptions, diffraction will set an upper limit on the width of the Si-O-Si angle distribution. In contrast, the quadrupolar asymmetry parameter, from which our Si-O-Si bond angle distribution is derived, provides a more direct probe of the Si-O-Si angle. We do note, however, that any additional structural asymmetries around the bridging oxygen may lead to a slight increase in

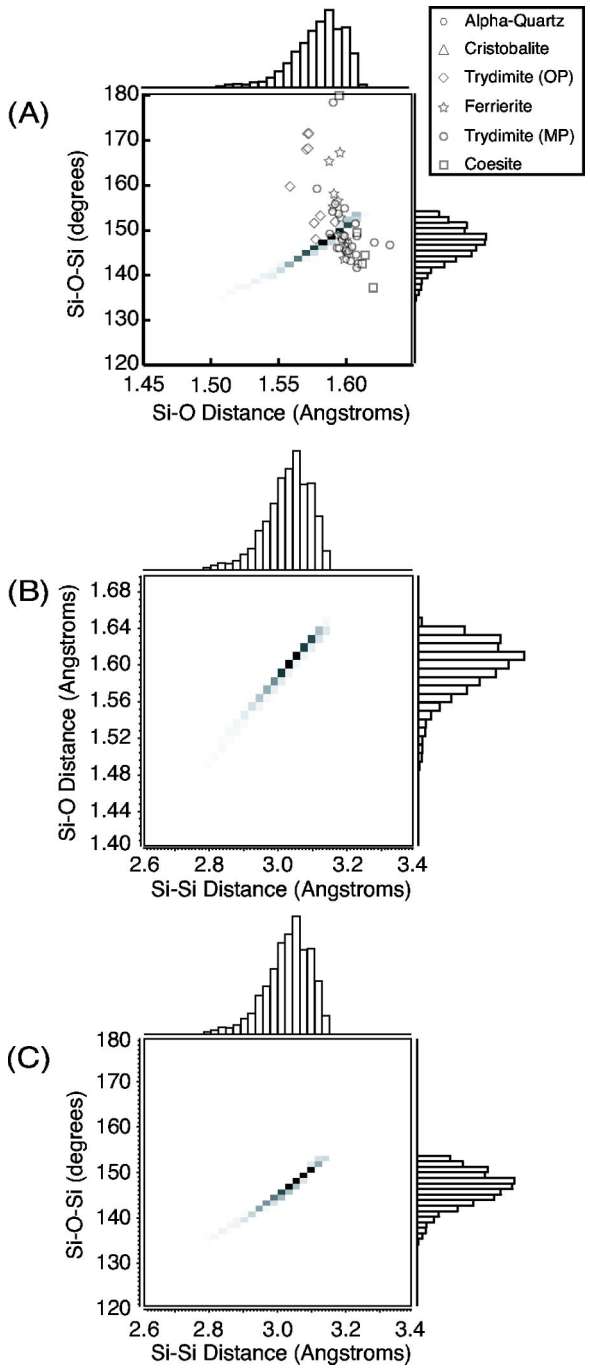

FIG. 3. Two-dimensional histograms of bridging oxygen structural parameters derived from NMR parameter distributions in Fig. 2. (a) The Si-O-Si angle versus the Si-O distance for silica glass (shown in black), and for various crystalline silica polymorphs; (b) the Si-O distance versus the Si-Si distance; and (c) the Si-O-Si angle versus the Si-Si distance.

TABLE I. Statistical parameters calculated from one-dimensional distributions measured in SiO_2 glass. The skew is calculated as the third moment about the mean. The covariances between C_q and η_q, C_q and δ_{cs}, and η_q and δ_{cs}, are $\sigma^2_{C_q,\eta_q}=0.0154$ MHz, $\sigma^2_{C_q,\delta_{cs}}=1.342$ MHz ppm, and $\sigma^2_{\eta_q,\delta_{cs}}=0.149189$ ppm, respectively. The covariances between Ω and d(Si-O), Ω and d(Si-Si), and d(Si-O) and d(Si-Si) are 0.0716 deg Å, 0.2519 deg Å, and 0.00128 Å^2, respectively.

	Mean	Mode	Median	Std. dev.	Skew
C_q	−5.08 MHz	−5.27 MHz	−5.14 MHz	0.372 MHz	0.893
η_q	0.150	0.137	0.143	0.0414	0.893
δ_{cs}	37.58 ppm	39.56 ppm	38.01 ppm	3.96 ppm	−0.570
Ω	146.6°	147.1°	146.9°	3.78°	−0.433
d(Si-O)	1.583 Å	1.589 Å	1.586 Å	0.0191 Å	−0.950
d(Si-Si)	3.030 Å	3.049 Å	3.041 Å	0.0670 Å	−0.811

the quadrupolar asymmetry parameter. Such an increase would be interpreted as a slightly lower Si-O-Si angle in our current analysis, and this effect may contribute to the strong decrease in the Si-O-Si distribution population at higher Si-O-Si angles. It is also worth noting, however, that our Si-O-Si angle distribution of silica glass is remarkably consistent with the one, also shown in Fig. 4(a), obtained from a molecular dynamics simulation, performed by Yuan and Cormack[41] when using a three-body potential of Vessal *et al.*[42]

Details on the Si-O-Si angle distribution in silica will also have implications for the ring size distribution. Silica glass with a high fictive temperature (T_f) has a more probable Si-O-Si angle near 141°, a greater presence of three and four member rings, and well-defined SiO_4 tetrahedra. In contrast, a lower T_f silica glass, such as the glass in this study, still includes well-defined SiO_4 tetrahedra, but the mean Si-O-Si angle increases, six member rings are more favored, and three and four membered rings are excluded.[43–47] The narrowness of the Si-O-Si angle distribution also has implications for the ring topology. Specifically, three member rings, with predicted Si-O-Si angles ranging from 128° to 136°, will be significantly less probable.[48–50] Conclusions regarding the occurrence of four member rings are less clear because the range of angles for these structures may overlap with angles expected for the more prevalent 5 or 6 member rings.[49–51]

The structure will have a pronounced effect on the physical properties of silica glass.[52] Although models of silica glass have been proposed with broad Si-O-Si bond angle distributions, narrow distributions consistent with our results have also been proposed that agree with the glass' physical properties, such as density.[44] A narrow bond angle distribution centered near 147° should not be problematic with respect to bond connectivity or strain because it is consistent with a ring topology dominated by 6 member rings and avoids smaller, less stable rings. It is noteworthy that β-cristobalite and HP-tridymite, each having densities nearly the same as silica glass, are composed entirely of six member rings and have Si-O-Si angles near 149°. This has led to the suggestion, supported by the present investigation, that structural similarities exist between these polymorphs of SiO_2 and silica glass.[44,53]

We also have found that the one-dimensional Si-O distance distribution has a mode of 1.59 Å and a standard deviation of 0.0191 Å. Although this mode is less than 1.605 Å obtained by diffraction methods,[54] it is still within the precision of our current calibration of Eqs. (2) and (3). The one-dimensional Si-Si distance distribution peaks at 3.05 Å, in reasonable agreement with diffraction measurements, and has a standard deviation of 0.067 Å. As seen in Fig. 3(a), the range of Si-O distances in silica glass is similar to those found in crystalline silica polymorphs. The Si-O and Si-Si distances are also within the range of values typically presented for SiO_2 glass,[55,54] and have overall distribution widths that are slightly narrower compared to the x-ray radial correlation function of silica glass, after taking the x-ray form factors and Q-space resolution into account. For comparison, the ^{17}O NMR derived Si-O and Si-Si distance distributions, convoluted with the proper x-ray form factors[56] and a step function with Q_{max} of 23.55 Å^{-1}, are shown in Fig. 4(b) along with the radial correlation function obtained from x-ray diffraction.[4,5] There is excellent agreement between the Si-O peaks at 1.6 Å, and, although the Si-Si contribution to the x-ray radial correlation function is wider than the NMR peak at 3 Å, this difference may be due to contributions from the first and second shell O−O distances which were not part of the x-ray convoluted NMR distance distribution.

In Fig. 3 we show, for the first time, the experimentally measured two-dimensional structural distributions in a glass. Strong nearly linear correlations among Si-O-Si angle, Si-O distance, and Si-Si distance in silica glass are observed. Most unexpected is the strong *positive* correlation between Si-O distance and Si-O-Si bond angle in silica glass, which is the opposite of that generally found in crystalline SiO_2 polymorphs,[57,58] as shown in Fig. 3(a). An increase in Si-O distance as the Si-O-Si angle increases, although not expected based on crystalline SiO_2 polymorphs or quantum chemical calculations for model clusters in the gas phase, is not without precedent. Recent molecular dynamics simulations of quartz by Kihara,[59] for example, suggests that with increasing temperature both the Si-O distance and Si-O-Si bond angle increase. Kihara found this result to be consistent with previous diffraction data after

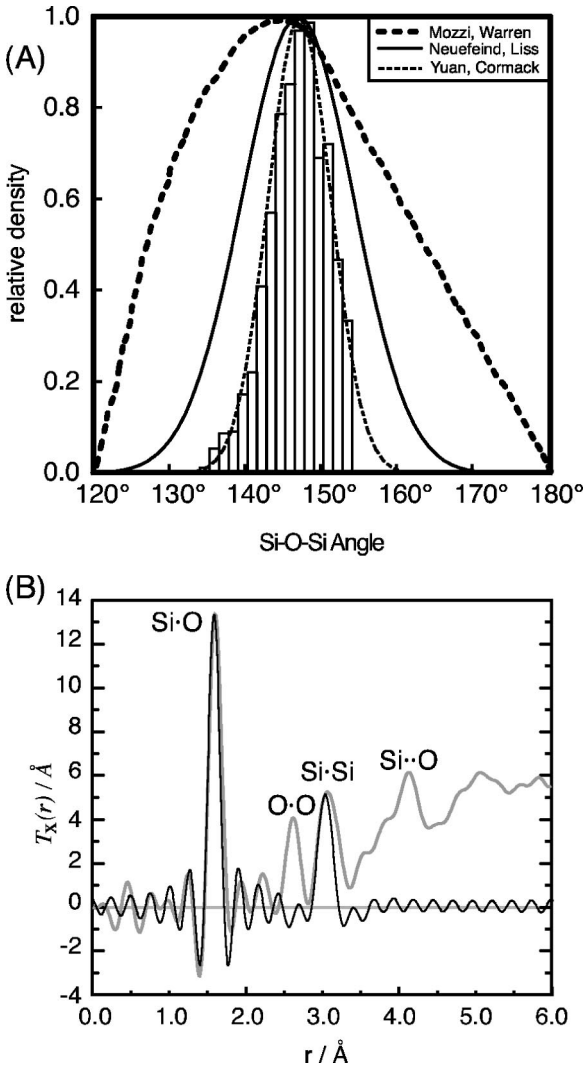

FIG. 4. (a) A comparison of the ^{17}O NMR derived Si-O-Si bond angle distribution with previous studies. The thick dashed line is the x-ray derived distribution of Mozzi and Warren (Ref. 3), the solid line is the x-ray derived distribution of Neuefeind and Liss (Refs. 4 and 5), and the thin dashed line is the distribution predicted by molecular dynamics simulations of Yuan and Cormack (Ref. 41) using the three-body potential from Vessal *et al.* (Ref. 42). (b) A comparison of the ^{17}O NMR derived Si-O and Si-Si distance distributions (shown as black line), after taking x-ray form factors and a Q_{max} of 23.55 Å^{-1} into account, with the total corrrelation function obtained from x-ray scattering (Refs. 4 and 5) (shown as a gray line).

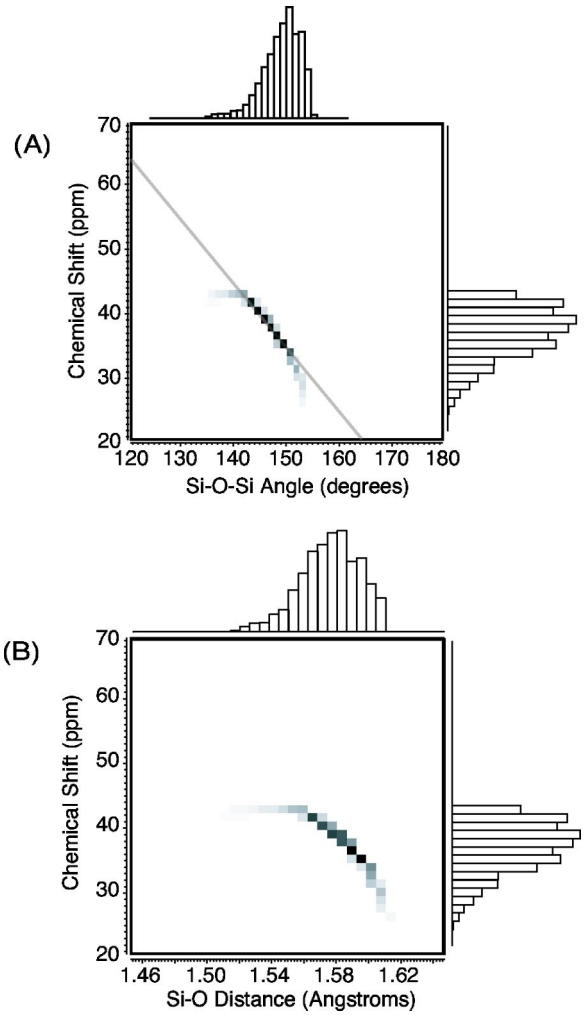

FIG. 5. Two-dimensional histograms showing the correlations between bridging oxygen ^{17}O chemical shift and (a) Si-O-Si angle and (b) Si-O distance, derived from the C_q and η_q data. The solid line in (a) is a least squares linear fit of the data, with a slope of –0.986 ppm/degree, an intercept of 182.17 ppm, and a linear correlation coefficient of $r^2 = 0.744$.

bond lengths were corrected for the librational motion of each silicate tetrahedra.[60] Similarly, a decrease in Si-O-Si angle and a decrease in Si-O distance has been proposed for low quartz under high pressure conditions, based on *ab initio* calculations.[61] It should be noted, however, that these calculated changes in Si-O bond distance are smaller than those described here for SiO_2 glass. Nonetheless, these observations suggest that the positive correlation observed through our ^{17}O NMR data may be the effect of trapped density fluctuations resulting from the disequilibrium nature of the glass.

Finally, we note that simple correlations between ^{17}O isotropic chemical shift and local structure around bridging oxygen have been more elusive.[19,40,62] The correlation between quadrupolar coupling constants and chemical shift observed in Fig. 2 is consistent with previous ^{17}O NMR measurements in silicates.[62,63] By using the derived structural distributions discussed above, we can consider the possible correlations between ^{17}O isotropic chemical shift, δ_{cs}, and the Si-O-Si angle or Si-O distance in SiO_2 glass. As shown in Fig. 5(a), a strong correlation is evident for the most probable Si-O-Si angles with δ_{cs} decreasing with an increasing Si-O-Si angle. The range of δ_{cs} values in SiO_2 glass is in much closer agreement with that proposed for ferrierite (28–42 ppm),[40,62] rather than that determined for coesite (40–60 ppm).[19] Recently, Loeser *et al.*[64] showed that δ_{cs} decreases linearly with increasing Si-O-Si in sodalites in some special cases. For Na, K-LSX hydrated zeolite they found a slope and intercept of −0.92 ppm/degree and 171 ppm, respectively, both in close agreement with the data

in Fig. 5(a). The range of values suggested by the *ab initio* calculations for the dimer $[(OH)_3O\text{-}Si\text{-}O\text{-}(OH)_3]$[65] (data not shown) is much smaller than that present in SiO_2 glass for this range of angles. As discussed by Xue and Kanzaki,[65] a wider range of values is expected if higher order structures are included beyond the first coordination sphere, and such structures are thought to account for the δ_{cs} values for sites in coesite.

IV. CONCLUSION

We have shown how the two-dimensional ^{17}O DAS solid-state NMR spectrum of silica glass can be analyzed to obtain two-dimensional histograms correlating the Si-O-Si angle with Si-O distance, Si-O-Si angle with Si-Si distance, and Si-O distance with Si-Si distance. This approach is general, and can be applied to measure the structural distributions around bridging oxygen in any ^{17}O enriched[66–68,40] crystalline or noncrystalline silicate.

The one-dimensional distance distributions obtained for silica glass with this approach are consistent, within the precision of the method, with the radial correlation function obtained from x-ray diffraction methods. The Si-O-Si angle distribution obtained, in contrast, is significantly narrower than those predicted from previous x-ray diffraction analyses of silica glass. This is not surprising, since Si-O-Si angle distribution determinations from diffraction data are obtained from structural modeling that is likely to be underconstrained.

The two-dimensional structural distributions measured here reveal an unexpected strong positive correlation between the Si-O-Si angle and Si-O distance in the glass, running opposite to the trend generally found in crystalline silica polymorphs. These observations may be the effect of trapped density fluctuations resulting from the disequilibrium nature of the glass. Future measurements on annealed samples could be useful for testing this hypothesis.

ACKNOWLEDGMENTS

We thank Jeff Allwardt for help in collecting ^{29}Si NMR spectra, Bob Jones for the EPMA analysis, and Chris Benmore and Joerg Neuefeind for helpful discussions. This material is based upon work supported by the National Science Foundation under Grants No. CHE 0111109 (PJG) and No. EAR 0104926 (JFS). Any opinions, findings and conclusions or recommendations expressed in this material are those of the author(s) and do not necessarily reflect the views of the National Science Foundation.

*Electronic address: grandinetti.1@osu.edu

[1] W. H. Zachariasen, J. Am. Chem. Soc. **54**, 3841 (1932).
[2] B. E. Warren, H. Krutter, and O. Morningstar, J. Am. Ceram. Soc. **19**, 202 (1936).
[3] R. L. Mozzi and B. E. Warren, J. Appl. Crystallogr. **2**, 164 (1969).
[4] J. Neuefeind and K.-D. Liss, Ber. Bunsenges. Phys. Chem. **100**, 1341 (1996).
[5] H. F. Poulsen, J. Neuefeind, H.-B. Neuman, J. R. Schneider, and M. D. Zeidler, J. Non-Cryst. Solids **188**, 63 (1995).
[6] P. A. V. Johnson, A. C. Wright, and R. N. Sinclair, J. Non-Cryst. Solids **58**, 109 (1983).
[7] D. I. Grimley, A. C. Wright, and R. N. Sinclair, J. Non-Cryst. Solids **119**, 49 (1990).
[8] E. Dupree and R. F. Pettifer, Nature (London) **308**, 523 (1984).
[9] R. Aujla, R. Dupree, I. Farnan, and D. Holland, Diffus. Defect Data **53**, 99 (1987).
[10] R. F. Pettifer, R. Dupree, I. Farnan, and U. Sternberg, J. Non-Cryst. Solids **106**, 408 (1988).
[11] F. Mauri, A. Pasquarello, B. G. Pfrommer, Y.-G. Yoon, and S. G. Louie, Phys. Rev. B **62**, R4786 (2000).
[12] L. F. Gladden, T. A. Carpenter, and S. R. Elliott, Philos. Mag. B **53**, L81 (1986).
[13] S. R. Elliott, J. Non-Cryst. Solids **123**, 149 (1990).
[14] J. A. Tossell and P. Lazzeretti, Chem. Phys. Lett. **112**, 205 (1987).
[15] J. A. Tossell and P. Lazzeretti, Phys. Chem. Miner. **15**, 564 (1988).
[16] C. G. Lindsay and J. A. Tossell, Phys. Chem. Miner. **18**, 191 (1991).
[17] U. Sternberg, Solid State Nucl. Magn. Reson. **2**, 181 (1993).
[18] X. Xue and M. Kanzaki, Solid State Nucl. Magn. Reson. **16**, 245 (2000).
[19] P. J. Grandinetti, J. H. Baltisberger, U. Werner, A. Pines, I. Farnan, and J. F. Stebbins, J. Phys. Chem. **99**, 12341 (1995).
[20] T. M. Clark and P. J. Grandinetti, Solid State Nucl. Magn. Reson.16, 55 (2000).
[21] K. E. Vermillion, P. Florian, and P. J. Grandinetti, J. Chem. Phys. **108**, 7274 (1998).
[22] T. M. Clark, P. J. Grandinetti, P. Florian, and J. F. Stebbins, J. Phys. Chem. B **105**, 12 257 (2001).
[23] T. M. Clark and P. J. Grandinetti, J. Phys.: Condens. Matter **15**, S2387 (2003).
[24] A. E. Geissberger and P. J. Bray, J. Non-Cryst. Solids **54**, 121 (1983).
[25] A. Bax, N. M. Szeverenyi, and G. E. Maciel, J. Magn. Reson. (1969-1992) **52**, 147 (1983).
[26] T. Terao, T. Fujii, T. Onodera, and A. Saika, Chem. Phys. Lett. **107**, 145 (1984).
[27] K. T. Mueller, B. Q. Sun, G. C. Chingas, J. W. Zwanziger, T. Terao, and A. Pines, J. Magn. Reson. (1969-1992) **86**, 470 (1990).
[28] P. Zhang, C. Dunlap, P. Florian, P. J. Grandinetti, I. Farnan, and J. F. Stebbins, J. Non-Cryst. Solids **204**, 294 (1996).
[29] P. Zhang, P. J. Grandinetti, and J. F. Stebbins, J. Phys. Chem. B **101**, 4004 (1997).
[30] I. Farnan, P. J. Grandinetti, J. H. Baltisberger, J. F. Stebbins, U. Werner, M. A. Eastman, and A. Pines, Nature (London) **358**, 31 (1992).
[31] Z. Yao, H.-T. Kwak, D. Sakellariou, L. Emsley, and P. J. Grandi-

netti, Chem. Phys. Lett. **327**, 85 (2000).
[32] S. Prasad, H. T. Kwak, T. Clark, and P. J. Grandinetti, J. Am. Chem. Soc. **124**, 4964 (2002).
[33] H.-T. Kwak, S. Prasad, Z. Yao, P. J. Grandinetti, J. R. Sachleben, and L. Emlsey, J. Magn. Reson. **150**, 71 (2001).
[34] M. A. Eastman, P. J. Grandinetti, Y. K. Lee, and A. Pines, J. Magn. Reson. (1969-1992) **98**, 333 (1992).
[35] K. T. Mueller, E. W. Wooten, and A. Pines, J. Magn. Reson. (1969-1992) **92**, 620 (1990).
[36] P. J. Grandinetti, J. H. Baltisberger, A. Llor, Y. K. Lee, U. Werner, M. A. Eastman, and A. Pines, J. Magn. Reson., Ser. A **103**, 72 (1993).
[37] S. Sen and J. F. Stebbins, J. Non-Cryst. Solids **188**, 54 (1995).
[38] D. R. Spearing, I. Farnan, and J. F. Stebbins, Phys. Chem. Miner. **19**, 307 (1992).
[39] R. Dupree, in *Structure and Imperfections in Amorphous and Crystalline* SiO_2, edited by R. Devine, J. P. Durand, and E. Dooryhee (Wiley, New York, 2000), pp. 107–120.
[40] L. M. Bull, B. Bussemer, T. Anupold, A. Reinhold, A. Samoson, J. Sauer, A. K. Cheetham, and R. Dupree, J. Am. Chem. Soc. **122**, 4948 (2000).
[41] X. Yuan and A. N. Cormack, J. Non-Cryst. Solids **319**, 31 (2003).
[42] B. Vessal, M. Amini, D. Fincham, and C. R. A. Catlow, Philos. Mag. B **60**, 753 (1989).
[43] R. LeParc, B. Champagnon, P. Guenot, and S. Dubois, J. Non-Cryst. Solids **293-295**, 366 (2001).
[44] L. W. Hobbs, C. E. Jesurum, V. Pulim, and B. Berger, Philos. Mag. A **78**, 679 (1998).
[45] H. Kakiuchida, K. Saito, and A. J. Ikushima, J. Appl. Phys. **94**, 1705 (2003).
[46] K. Vollmayr, W. Kob, and K. Binder, Phys. Rev. B **54**, 15 808 (1996).
[47] R. Brüning and D. Cottrell, J. Non-Cryst. Solids **325**, 6 (2003).
[48] A. Pasquarello and R. Car, Phys. Rev. Lett. **80**, 5145 (1998).
[49] J. P. Rino, I. Ebbsjö, R. K. Kalia, A. Nakano, and P. Vashishta, Phys. Rev. B **47**, 3053 (1993).
[50] T. Uchino, . Tokuda, and T. Yoko, Phys. Rev. B **58**, 5322 (1998).
[51] T. Uchino, Y. Kitagawa, and T. Yoko, Phys. Rev. B **61**, 234 (2000).
[52] A. Agarwal and M. Tomozawa, J. Non-Cryst. Solids **209**, 166 (1997).
[53] D. A. Keen and M. T. Dove, J. Phys.: Condens. Matter **11**, 9263 (1999).
[54] A. C. Wright, J. Non-Cryst. Solids **179**, 84 (1994).
[55] Y. Xianglong and A. N. Cormack, J. Non-Cryst. Solids **283**, 69 (2001).
[56] D. Waasmaier and A. Kirfel, Acta Crystallogr., Sect. A: Found. Crystallogr. **51**, 416 (1995).
[57] M. D. Newton and G. V. Gibbs, Phys. Chem. Miner. **6**, 221 (1980).
[58] G. V. Gibbs, Am. Mineral. **67**, 421 (1982).
[59] K. Kihara, Phys. Chem. Miner. **28**, 365 (2001).
[60] R. T. Downs, G. V. Gibbs, K. L. Bartelmehs, and M. B. Boisen, Am. Mineral. **77**, 751 (1992).
[61] G. V. Gibbs, K. M. Rosso, D. M. Teter, M. B. Boisen, and M. S. T. Bukowinski, J. Mol. Struct. **485–486**, 13 (1999).
[62] M. Profeta, F. Mauri, and C. J. Pickard, J. Am. Chem. Soc. **125**, 541 (2003).
[63] S. K. Lee, J. F. Stebbins, J. C. A. Weiss, and R. J. Kirkpatrick, Chem. Mater. **15**, 2605 (2003).
[64] T. Loeser, D. Freude, G. Mabande, and W. Schwieger, Chem. Phys. Lett. **370**, 32 (2003).
[65] X. Xue and M. Kanzaki, Phys. Chem. Miner. **26**, 14 (1998).
[66] S. Yang, K. D. Park, and E. Oldfield, J. Am. Chem. Soc. **111**, 7278 (1989).
[67] J. A. Abys, D. M. Barnes, S. Feller, G. B. Rouse, and W. M. Risen, Mater. Res. Bull. **15**, 1581 (1980).
[68] L. M. Bull, A. K. Cheetham, T. Anupold, A. Reinhold, A. Samoson, J. Sauer, B. Bussemer, Y. Lee, S. Gann, J. Shore *et al.*, J. Am. Chem. Soc. **120**, 3510 (1998).